Title
A minK-HERG complex regulates the cardiac potassium current I(Kr).

Journal
Nature, 388(6639)

ISSN
0028-0836

Authors
McDonald, TV
Yu, Z
Ming, Z
et al.

Publication Date
1997-07-01

DOI
10.1038/40882

A minK–HERG complex regulates the cardiac potassium current I_{Kr}

Thomas V. McDonald, Zhihui Yu, Zhen Ming, Eugen Palma, Marian B. Meyers, Ke-Wei Wang*, Steve A. N. Goldstein* & Glenn I. Fishman

Section of Molecular Cardiology, Albert Einstein College of Medicine, 1300 Morris Park Avenue, Bronx, New York 10461, USA

* Departments of Pediatrics and Cellular and Molecular Physiology,
The Boyer Center for Molecular Medicine, Yale University School of Medicine, New Haven, Connecticut 06536, USA

MinK is a widely expressed protein of relative molecular mass ~15K that forms potassium channels by aggregation with other membrane proteins[1–3]. MinK governs ion channel activation[4], regulation by second messengers[5,6], and the function and structure of the ion conduction pathway[7,8]. Association of minK with a channel protein known as KvLQT1 produces a voltage-gated outward K^+ current (I_{sK}) resembling the slow cardiac repolarization current (I_{Ks})[9,10]. *HERG*, a human homologue of the *ether-a-go-go* gene of the fruitfly *Drosophila melanogaster*, encodes a protein that produces the rapidly activating cardiac delayed rectifier (I_{Kr})[11,12]. These two potassium currents, I_{Ks} and I_{Kr}, provide the principal repolarizing currents in cardiac myocytes for the termination of action potentials[13,14]. Although heterologously expressed HERG channels are largely indistinguishable from native cardiac I_{Kr}, a role for minK in this current is suggested by the diminished I_{Kr} in an atrial tumour line subjected to minK antisense suppression[15]. Here we show that HERG and minK form a stable complex, and that this heteromultimerization regulates I_{Kr} activity. MinK, through the formation of heteromeric channel complexes, is thus central to the control of the heart rate and rhythm.

We studied a clonal line of Chinese hamster ovary (CHO) cells stably expressing HERG (CHO-HERG) by whole-cell voltage clamp. CHO-HERG cells showed voltage-gated K^+ currents typical of human I_{Kr} which were absent from untransfected CHO cells (Fig. 1a). HERG currents showed voltage-dependent activation and deactivation, inward rectification at positive potentials, and sensitivity to E4031 like that of endogenous cardiac I_{Kr} (refs 13, 14) and HERG-K^+ channels expressed in *Xenopus* oocytes[11,12]. CHO cells transfected with minK alone gave no voltage-gated currents (Fig. 1b; $n = 6$), as already reported[16]. We confirmed the activity of minK by co-expression with KvLQT1, which produced I_{Ks}-like currents (data not shown) as expected[9,10]. When minK was co-expressed in CHO- HERG cells, an I_{Kr}-like current similar to HERG, but larger, was seen (Fig. 1c).

HERG and HERG–minK current densities were quantified by measuring maximal tail currents at –40 mV after a 2-s depolarizing test pulse to +60 mV. Currents were normalized for plasma membrane surface area by cell capacitance. Co-expression of minK and HERG resulted in a doubling of the K^+ current density (HERG, 12.8 ± 1.6 pA per pF, $n = 55$; HERG–minK, 24.0 ± 3.45 pA per pF, $n = 39$; $P < 0.001$) (Fig. 2a). To assess the specificity of this response, the effect of D77N-minK on HERG currents was studied. D77N-minK is expressed on the surface of *Xenopus* oocytes as is wild type, but it produces no I_{sK} current[2]. When D77N-minK was co-expressed with HERG, there was no increase in K^+ current (tail current density, 12.9 ± 1.7 pA per pF, $n = 37$; P, NS).

Whole-cell current is described by the equation $I = n(P_o)i$, where I is the measured current, n the number of functional channels, P_o the probability of channel opening, and i the unitary channel current amplitude. Thus, an increase in current density must be due to changes in channel gating kinetics (P_o), i, n, or to changes in membrane surface area. First, the gating kinetics of HERG and HERG–minK channels were compared. MinK produced a hyper- polarizing shift of 6–10 mV in the voltage dependence of activation (Fig. 2b). The current–voltage relationship (Fig. 2c) showed a hyperpolarizing shift of similar magnitude at voltages more negative than +20 mV and at more positive potentials, up to an 18-mV shift in negative slope conductance as a result of increased steady- state inactivation (Fig. 2d). These results indicated that minK produced an increase in the voltage sensitivity of activation and inactivation at intermediate voltages. These changes in gating could not, however, account for increased maximal current densities. No significant differences were measured for time constants of activation at +60 mV or deactivation at –40 mV between

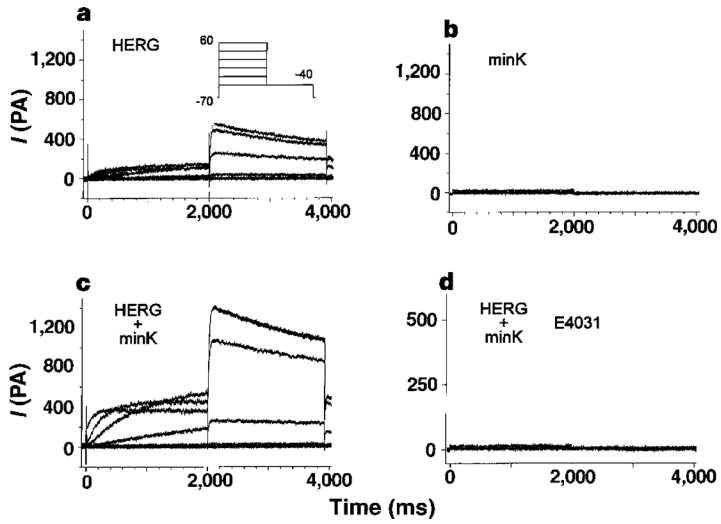

Figure 1 Functional expression of HERG and HERG with minK. **a**, A CHO-HERG cell showing voltage-gated K^+ current typical for I_{Kr}. The holding potential was –70 mV, cells were depolarized to potentials between 0 and +60 mV and tail currents measured during repolarization to –40 mV. **b**, A CHO cell transiently transfected with minK showing no voltage-gated currents. **c**, A CHO-HERG cell transiently transfected with minK showing HERG–minK, I_{Kr}-like K^+ currents. **d**, E4031 at 500 nM completely blocks all voltage-activated K^+ conductance in a cell expressing minK and HERG.

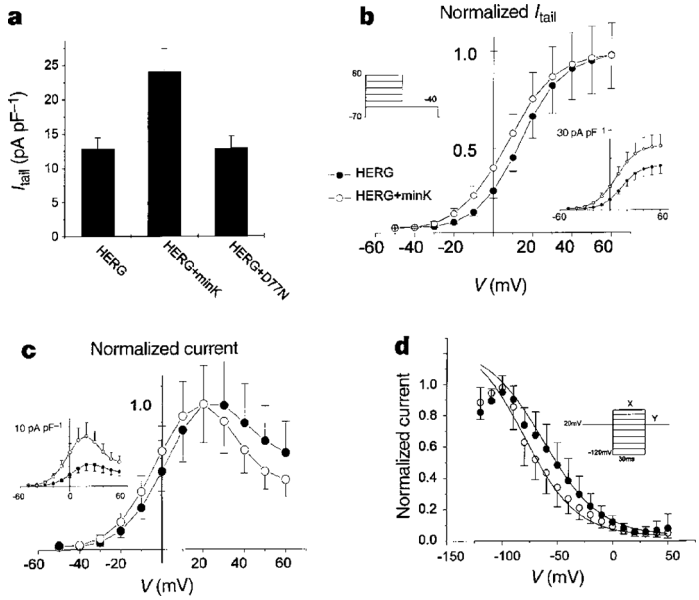

Figure 2 MinK alters functional expression of HERG in CHO cells. **a**, HERG current density is augmented by minK but not D77N-minK. The bar graph summarizes current densities for CHO-HERG cells (n = 55 cells), CHO-HERG cells transfected with wild-type minK (n = 39 cells), or CHO-HERG cells transfected with D77N- minK (n = 37 cells). Peak tail currents were measured as for Fig.1 and normalized for cell capacitance. **b**, Voltage–activation curves; normalized peak tail current density at –40 mV was plotted against test potential, demonstrating a left shift in voltage-dependent activation. Current density is greater for HERG–minK at all potentials that activate current (inset: data plotted without normalization). Data were fitted to the Boltzmann relation, $y = 1/(1 + \exp[(V_h – V)/k])$, where V is the test potential, V_h the potential at half-maximal activation (+12 mV for HERG and +6 mV for HERG–minK) and k is the slope factor (11 mV for both). **c**, Current–voltage relation for HERG and HERG-minK cells. Normalized current during depolarization is plotted against the membrane potential. There is a hyperpolarizing shift in voltage dependence that is most pronounced at potentials greater than +20 mV. Current density is greater for HERG–minK than HERG alone at all voltages (inset: data plotted without normalization). **d**, Steady-state inactivation[30] was assessed by brief steps to various hyperpolarized potentials from +20 mV; the plot shows peak current released from inactivation at +20 mV against test potential. Inset shows voltage pulse protocol with X showing the voltage steps and Y indicating where current was measured.

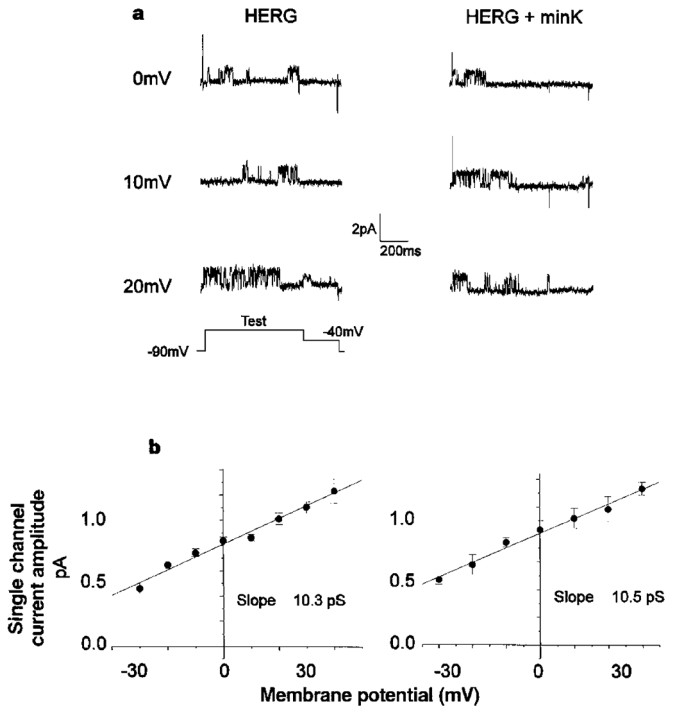

Figure 3 Single-channel currents from HERG and HERG–minK. **a,** Cell-attached patch recordings of single K^+ channel currents form CHO-HERG cells. Voltage protocol is shown below the current traces. **b**, Single-channel current–voltage curves showing unitary conductances for HERG and HERG–minK.

HERG and HERG–minK channels (τ_{act}: HERG, 282 ± 72 ms, n = 16; HERG– minK, 246 ± 38 ms, n = 17, P is NS; τ_{fast} deactivation: HERG, 477 ± 78 ms, n = 16; HERG–minK, 428 ± 64 ms, n = 17, P is NS).

As changes in gating kinetics did not explain the increased current density, single channel conductances were determined. Unitary conductances for HERG and HERG–minK channels between –30 and +40 mV were 10.3 ± 0.5 pS (n = 8) and 10.6 ± 0.4 pS (n = 14), respectively (Fig. 3). Thus, changes in i also failed to account for increased whole-cell current density. Neither did changes in membrane area lead to increased currents; the surface areas of cells expressing HERG or HERG–minK were not significantly different (34.1 ± 2.7 pF, n = 50 and 29.7 ± 2.7 pF, n = 46, respectively). Therefore, a change in the number of functional channels in the plasma membrane must underlie the effect of minK on HERG currents. These currents appear to result from HERG–minK channels rather than induction of non-HERG K^+ conductances because E4031, a specific blocker of I_{Kr}, abolished all voltage-gated K^+ currents in HERG- and HERG–minK-expressing cells (Fig. 1d) at concentrations used to distinguish between I_{Kr} and I_{Ks} (0.5 and 1.0 μ,M)[13].

To assess whether minK influenced HERG by direct physical contact and formation of a stable heteromeric complex, the proteins were epitope-tagged for protein analysis. A c-Myc epitope at the carboxy terminus of HERG had no measurable effect on channel currents (data not shown). Similarly, a haemagglutinin (HA) epitope between minK amino acids 22 and 23 was also well tolerated, as shown before[5], and did not alter its augmentation of HERG currents or formation of functional I_{Ks} channels with KvLQT1 (data not shown). Expression of HA–minK produced three specific bands corresponding to relative molecular masses (M_r) of ~15K–25K, which represent unmodified and glycosylated forms of minK (Fig. 4a), as expected[4]. Expression of HERG–Myc yielded a single band of M_r ~ 130K, consistent with the predicted mobility of HERG (Fig. 4a).

When HERG–Myc and HA–minK were co-expressed, immune-precipitation of either protein led to recovery of both channel subunits (Fig. 4b,c; n = 3). Although D77N–minK did not augment HERG currents (Fig. 2a), HA–D77N-minK did associate with HERG to form a stable complex like the wild-type protein (Fig. 4c, lane 4; n = 2). The association between HERG and minK was specific; when Myc-tagged connexin 43 (Cx43-Myc), an unrelated membrane channel subunit, was co-expressed with both HA–minK and

HERG–Myc, immunoprecipitation with anti-HA antibody recovered only HERG and no Cx43 (Fig. 4d).

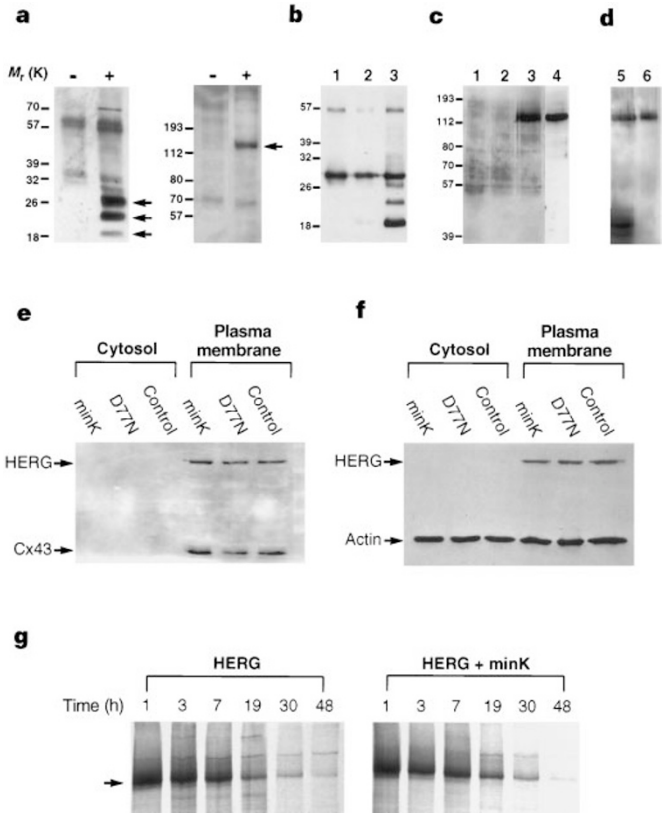

Figure 4 Association of minK and HERG**. a**, Expression of epitope-tagged constructs. Cell lysates probed with anti-HA, showing three bands corresponding to native and glycosylated forms of minK (left), or with anti-Myc, showing a single band of ~130K as predicted for HERG protein (right). Control lanes (–) are lysates from untransfected cells. **b,** Co-immunoprecipitation of minK with HERG. Lysates were immunoprecipitated with anti-Myc antibody followed by SDS–PAGE and detection with anti-HA. Lanes: 1, untransfected cells; 2, cells transfected with HERG–Myc; 3, cells transfected with HERG–Myc and HA–minK. **c**, Co- immunoprecipitation of HERG with minK or D77N-minK. Lysates were immuno-precipitated with anti-HA antibody followed by SDS–PAGE and detection with anti-Myc antibody. Lanes: 1, untransfected cells; 2, cells transfected with HA– minK; 3, cells transfected with HA-minK and HERG-minK and HERG–Myc; 4, cells transfected with HA–D77N-minK and HERG—Myc. **d**, Specificity of HERG–minK interaction. Lane 1, Lysate from cells transfected with HA-minK, HERG–Myc, and Cx43-myc probed with anti-cmyc monoclonal antibody capable of detecting both HERG-Myc and Cx43-myc. Lane 2, same lysate immunoprecipitated with anti-HA antibody, followed by SDS–PAGE and detection with peroxidase-conjugated anti- Myc antibody, showing recovery of only HERG–Myc. **e**, Epitope-tagged HERG localizes to the plasma membrane. CHO cells were transfected with HERG–Myc either alone (control) or in combination with HA–minK or HA–D77N-minK. Cx43– Myc was included in all transfections. Lysates were fractionated into plasma cytosolic and membrane fractions. HERG–Myc and Cx43–Myc were recovered exclusively in the membrane fraction. Co-expression of minK or D77N-minK did not affect the abundance of HERG (n = 3). **f**, CHO-HERG cells stably expressing wild-type HERG were fractionated as described and detected with antisera against HERG. Unlike actin, HERG localized exclusively in the membrane fraction. Co-expression of HA–minK or HA–D77N-minK did not affect the abundance of HERG (n = 3). **g**, Pulse-chase analysis. The rate of degradation of metabolically labelled HERG was not significantly different in cells transfected with HERG–Myc alone or in combination with minK.

Although co-expression of HERG and minK increased the number of functional channels, it did not alter the amount of HERG protein on the cell surface. Western blot analysis was performed on membrane and cytosolic/microsomal fractions prepared from CHO cells transiently transfected with HERG-Myc and Cx43-Myc, either alone or in combination with HA–minK or HA– D77N-minK. In each case, all detectable HERG–Myc was recovered in the membrane fraction and the abundance of HERG–Myc (and Cx43-Myc) was unaffected by co-expression of HA–minK or HA– D77N-minK (Fig. 4e; *n* = 3). The same results were obtained when either HA–minK or HA–D77N-minK was expressed in the stable CHO-HERG cell line;

neither the membrane localization of HERG nor its level of expression was affected (Fig. 4f). Co-expression of minK with HERG also did not protect HERG from degradation. Pulse-chase analysis showed time constants of degradation of ~11.2 h and 11.6 h for HERG in the absence and presence of minK, respectively (Fig. 4g; $n = 2$).

Our results show that minK physically associates with HERG and that the interaction leads to increased I_{Kr} current density. The fact that both non-glycosylated and glycosylated forms of minK bind to HERG suggests that association takes place early in the protein synthesis and trafficking pathway, probably in the endoplasmic reticulum. As minK increases the number of functional HERG channels in the plasma membrane but does not alter cell-surface expression of the HERG protein, minK appears to increase the active fraction in a membrane pool containing active and dormant channels. This type of shift in channel activity may underlie upregulation of minK function in oocytes after treatment with cyclic AMP1. Similarly, cAMP has been shown to regulate the proportion of functional nicotinic acetylcholine receptor channels in chick ciliary ganglion cells[17]. Such mode switching is reminiscent of the gating behaviour seen in RCK4 K^+ channels, where a fraction of channels in oocyte patches fail to open with depolarization when external K^+ is removed[18].

The consequences of minK interaction with KvLQT1 and HERG are surprisingly similar. We have shown here that minK alters HERG channel gating kinetics and increases macroscopic I_{Kr} current density. By an as-yet unknown mechanism, minK also acts on KvLQT1 to alter its gating kinetics (to those characteristic of I_{Ks}) and to increase macroscopic current[9,10]. Although HERG produces I_{Kr}-like currents when expressed alone whereas KvLQT1 strictly requires minK to create recognizable I_{Ks} channels, this may be a quantitative rather than a qualitative difference. In this respect, it is notable that D77N-minK fails to augment I_{Kr} currents even though it physically associates with HERG protein (Figs 2a, 4c), just as it fails to produce I_{Ks} currents but can compete with wild-type minK when co-expressed in *Xenopus* oocytes[2]. This suggests that similar molecular features of minK are important for influencing the function of HERG and KvLQT1.

Inasmuch as minK is required for I_{Ks} and alters I_{Kr}, its expression and modulation by second messengers[5,6] will play a central role in determining the amount and character of the K^+ conductances in individual cardiac myocytes. Moreover, expression of minK, HERG, KvLQT1 and other K^+ channel proteins is region-specific in the heart and varies in pathological states, producing spatial heterogeneity in current densities and phenotypes[19,20]. Mutations in KvLQT1 and HERG produce hereditary long-QT syndrome (LQTS) by decreasing I_{Ks} and I_{Kr} (refs 21, 22), so minK should be expected to act as a modifier of genetically determined LQTS. As HERG has also been implicated in acquired arrhythmias[11,23], minK may be involved in susceptibility to acquired LQTS and pro- arrhythmic drug phenomena. In the mouse, disruption of the minK gene results in *shaker/waltzer* behaviour and hair-cell degeneration[24]. This null phenotype suggests an association between mutations in minK and Jervell and Lange–Nielsen syndrome, an autosomal recessive form of LQTS that is associated with deafness[23].

These results indicate a broad role for minK in determining the functional expression of delayed rectifier K^+ currents in the heart. The physical and functional interaction of minK with two diverse K^+ channel types (KvLQT1 and HERG) and its wide tissue distribution (heart, ear, kidney, pancreas, T cells and gastrointestinal tract)[25–28] suggest that the role of minK in normal physiology and disease pathogenesis may be even more extensive.

Methods

Plasmid construction and transfections. HERG was epitope-tagged by replacing the three C-terminal amino acids of the wild-type protein with ISMEQKLISEEDLN, derived from the c-myc gene recognized by monoclonal antibody 9E10. Construction of HA-tagged minK and D77N-minK have been described[1,2]. CHO cells stably expressing HERG were obtained by transfection with a pCI-based vector carrying HERG and selection with G418. Transient transfections were carried out by electroporation with the indicated minK constructs together with green fluorescent protein.

Electrophysiology. Cells were studied on an inverted microscope equipped with epifluorescence optics for GFP detection and electrophysiology experiments. Whole-cell voltage clamp was done with an internal solution of KCl 120 mM, $MgCl_2$ 2 mM, $CaCl_2$ 0.5 mM, EGTA 5 mM, ATP-Mg_4 4 mM, HEPES 10 mM (pH 7.2; osmolality, 280 ± 10 mOsm). External bath solution consisted of NaCl 150 mM, $CaCl_2$ 1.8 mM, KCl 4 mM, $MgCl_2$ 1 mM, glucose 5 mM, HEPES 10 mM (pH 7.4; osmolality, 320 ± 10 mOsm). Experiments were done at room temperature. On-cell and excised patch configuration was used to study single HERG channels. Cells were bathed in KCl 120 mM, NaCl 10 mM, $MgCl_2$ 2 mM, HEPES 10 mM (pH 7.4), glucose 5 mM. Signals were analogue-filtered at 2,000 Hz and sampled at 5–10 kHz. Amplitude histograms at each membrane potential were constructed to obtain single-channel conductance. Data were analysed using electrophysiology software (pClamp, Axon Instruments).

Protein analysis. Transfected cells were lysed in Tris lysis buffer (0.15 M NaCl, 1% NP-40, 1% CHAPS, 20 mM NaF, 10 mM Na_3VO_4, 1 mM PMSF and 50 mM Tris, pH 7.4). Lysates were cleared by centrifugation at 10,000g for 30 s. For direct immunoblot analysis, samples were separated by SDS–PAGE and epitope-tagged proteins detected with appropriate monoclonal antibodies conjugated to horseradish peroxidase (Boehringer Mannheim). For detection of untagged HERG, membranes were incubated with rabbit anti-HERG polyclonal antisera[29], followed by horseradish peroxidase-conjugated protein A. Lysates were immunoprecipitated with either 5 μ,g anti-HA 12CA5 or 3 μ,g anti-Myc 9E10 monoclonal antibody for 2 h at 4 °C, followed by incubation with protein G–Sepharose for 1 h at 4 °C. For pulse-chase analysis, cells were labelled for 30 min with ^{35}S-methionine/cysteine, chased in medium with excess unlabelled methionine/cysteine for varying times and collected by detergent lysis. After immunoprecipitation and SDS–PAGE, gels were visualized by fluorography and quantified by densitometry (Molecular Analysis, Biorad). For subcellular fractionation, adherent cells were detached by incubation with EDTA and gently disrupted by Dounce homogenization. Cellular lysates were layered on 45% sucrose cushions and membrane and cytosolic/ microsomal fractions recovered after centrifugation at 7,000g for 20 min.

Received 16 January; accepted 12 May 1997.

1. Blumenthal, E. M. & Kaczmarek, L. K. The minK potassium channel exists in functional and nonfunctional forms when expressed in the plasma membrane of *Xenopus* oocytes. *J. Neurosci*. **14**, 3097–3105 (1994).
2. Wang, K.-W. & Goldstein, S. A. N. Subunit composition of minK potassium channels. *Neuron* **14**, 1303–1309 (1995).
3. Tai, K. K., Wang, K. W. & Goldstein, S. A. N. MinK potassium channels are heteromultimeric complexes. *J. Biol. Chem*. **272**, 1654–1658 (1997).
4. Takumi, T. et al. Alteration of channel activities and gating by mutations of slow I_{sK} potassium channel. *J. Biol. Chem*. **2266**, 22192–22198 (1991).
5. Blumenthal, E. M. & Kaczmarek, L. Modulation by cAMP of a slowly activating potassium channel expressed in *Xenopus* oocytes. *J. Neurosci*. **12**, 290–295 (1992).
6. Busch, A. E., Kavanaugh, M. P., Varnum, J. P. & Adelman, J. P. Regulation by second messengers of the slowly activating, voltage-dependent potassium current expressed in *Xenopus* oocytes. *J. Physiol.* **450**, 491–502 (1992).
7. Goldstein, S. A. N. & Miller, C. Site-specific mutations in a minimal voltage-dependent K+ channel alter ion selectivity and open-channel block. *Neuron* **7**, 403–408 (1991).
8. Wang, K. W., Tai, K. K. & Goldstein, S. A. N. MinK residues line a potassium channel pore. *Neuron* **16**, 571–577 (1996).
9. Sanguinetti, M. C. et al. Coassembly of KVLQT1 and minK (IsK) proteins to form cardiac I_{Ks} potassium channel. *Nature* **384**, 80–83 (1996).
10. Barhanin, J. et al. K_VLQT1 and IsK (minK) proteins associate to form I_{Ks} cardiac potassium current.

Nature **384**, 80–83 (1996).
11. Sanguinetti, M. C., Jiang, C., Curran, M. E. & Keating, M. T. A mechanistic link between an inherited and an acquired cardiac arrhythmia: *HERG* encodes the I_{Kr} potassium channel. *Cell* **81**, 299–307 (1995).
12. Trudeau, M. C., Warmke, J. W., Ganetzky, B. & Robertson, G. A. *HERG*, a human inward rectifier in the voltage-gated potassium channel family. *Science* **269**, 92–95 (1995).
13. Sanguinetti, M. C. & Jurkiewicz, N. K. Two components of the delayed rectifier K^+ current: differential sensitivity to block by class III antiarrhythmic agents. *J. Gen. Physiol*. **96**, 195–215 (1990).
14. Sanguinetti, M. C. & Jurkiewicz, N. K. Delayed rectifier outward K^+ current is composed of two currents in guinea pig atria cells. *Am. J. Physiol*. **26**0, H393–H399 (1991).
15. Yang, T., Kupershmidt, S. & Roden, D. M. Anti-minK antisense decreases the amplitude of the rapidly activating cardiac delayed rectifier K+ current. *Circ. Res*. **77,** 1246–1253 (1995).
16. Lesage, F. et al. Are *Xenopus* oocytes unique in displaying functional IsK channel heterologous expression? *Receptors and Channels* **1**, 143–152 (1993).
17. Margiotta, J. F., Berg, D. K. & Dionne, V. E. Cyclic AMP regulates the proportion of functional acetylcholine receptors on chicken cilliary ganglion neurons. *Proc. Natl Acad. Sci. USA* **84**, 8155–8159 (1987).
18. Pardo, L. A. et al. Extracellular K+ specifically modulates a brain K+ channel. *Proc. Natl Acad. Sci. USA* **89**, 2466–2470 (1992).
19. Brahmajothi, M. V. et al. In situ hybridization reveals extensive diversity of K+ channel mRNA in isolated ferret cardiac myocytes. *Circ. Res*. **78**, 1083–1089 (1996).
20. Choy, A.-M. J., Kupershmidt, S., Lang, C. C., Pierson, R. N. & Roden, D. M. Regional expression of HERG and KVLQT1 in heart failure. *Circulation* **94**, 1–I164 (1996).
21. Curran, M. E. et al. A molecular basis for cardiac arrhythmia: *HERG* mutations cause long QT syndrome. *Cell* **80**, 795–803 (1995).
22. Wang, Q. et al. Positional cloning of a novel potassium channel gene: KVLQT1 mutations cause cardiac arrhythmias. *Nature Genet*. **12**, 17–25 (1996).
23. Roden, D. M. et al. Multiple mechanisms in the long-QT syndrome: Current knowledge, gaps, and future directions. *Circ. Res.* **94**, 1996–2012 (1996).
24. Vetter, D. E. et al. Inner ear defects induced by null mutation of the *isk* gene. *Neuron* **17**, 1251–1264 (1996).
25. Sugimoto, T. et al. Immunohistochemical study of a rat membrane protein which induces a selective potassium permeation: its localization in the apical membrane portion of epithelial cells. *J. Membr. Biol*. **113**, 39–47 (1990).
26. Sakagami, M. et al. Cellular localization of rat Isk protein in the stria vascularis by immunohisto-chemical observation. *Hearing Res*. **56**, 168–172 (1991).
27. Freeman, L. C. & Kass, R. S. Expression of a minimal K^+ channel protein in mammalian cells and immunolocalization in guinea pig heart. *Circ. Res*. **73**, 968–973 (1993).
28. Attali, B. et al. Cloning, functional expression, and regulation of two K^+ channels in human T lymphocytes. *J. Biol. Chem.* **267**, 8650–8657 (1992).
29. Pond, A. L., Petrecca, K., Van Wagoner, D. R., Shrier, A. & Nerbonne, J. M. Distinct isoforms of ERG expressed in rat and human heart. *Circ. Res.* (submitted).
30. Smith, P. L., Baukrowitz, T. & Yellen, G. The inward rectification mechanism of the HERG cardiac potassium channel. *Nature* **379**, 833–836 (1996).

Acknowledgements. We thank G. Robertson for HERG cDNA, J. Nerbonne and A. Pond for HERG antisera, K. Sawada for E4031, and V. S. Srinivas for technical assistance. This work was supported by funds from the AECOM Molecular Cardiology Endowment to T.V.M., M.B.M. and G.I.F., and by grants to G.I.F. from the American Heart Association (Established Investigator) and the Council for Tobacco Research and to S.A.N.G. from the NIH-NIGMS and Donaghue Foundation.

Correspondence and requests for materials should be addressed to T.V.McD. (e-mail: mcdonald@aecom.yu.edu).